Preliminary analysis of the ICRF launcher for DTT

Fusion Engineering and Design 191 (2023) 113788

Contents lists available at ScienceDirect

Fusion Engineering and Design

journal homepage: www.elsevier.com/locate/fusengdes

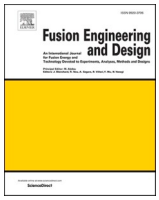

Preliminary analysis of the ICRF launcher for DTT

F. Mirizzi [a,b,*], S. Ceccuzzi [b,d], B. Baiocchi [c], A. Cardinali [d], G. Di Gironimo [a,b,e], G. Granucci [c], D. Mascali [f], G. Mauro [f], D. Milanesio [g], A. Pidatella [f], C. Ponti [h], G.L. Ravera [d], G. Torrisi [f], A.A. Tuccillo [a,b], G. Vecchi [g]

[a] Create Consortium Napoli, Italy
[b] DTT S.C. a r.l. Frascati, Italy
[c] CNR–ISTP, Milano, Italy
[d] ENEA Frascati, Italy
[e] Università di Napoli Federico II, Napoli, Italy
[f] INFN–LNS, Catania, Italy
[g] Politecnico di Torino, Torino, Italy
[h] Università Roma Tre, Roma, Italy

ARTICLE INFO

Keywords:
Divertor Tokamak Test (DTT)
ICRF systems
ICRF launcher
Current straps

ABSTRACT

The paper reports the preliminary analysis of different typologies of ICRH launchers for chosing the most efficient solution for the ICRH system of the Divertor Tokamak Test facility (DTT), designed by the Italian DTT Limited Liability Consortium (S.C. a r.l.). In its final configuration this system will couple to the DTT plasma a nominal power of 6 MW in the 60 – 90 MHz frequency range by means of four launchers. This very preliminary analysis has been done with the ANSYS HFSS code.

1. Introduction

The Divertor Tokamak Test (DTT) is a new facility [1] designed by the Italian DTT Limited Liability Consortium (S.C. a r.l.) aimed at validating an integrated solution for the power exhaust in view of DEMO [2]. This device, which main parameters are listed in Table 1, has now entered the realisation phase at the ENEA Frascati Research Centre.

DTT will be powered by 45 MW of additional heating power [3], mostly EC at 170 GHz, and negative NBI. It will be also provided with an ICRF system [4] that shall couple to the plasma a power of 6 MW in the 60–90 MHz frequency range by means of four launchers. The conceptual design of this system, having a modular configuration (Fig. 1) and powered by four high frequency generators, each one with an output power of 1.2 MW, has been already completed.

Significant efforts have been dedicated to the identification of the most suitable launcher concepts for mitigating the input reflection coefficient of strap arrays and the high electric fields within the launcher box and immediately in front of it.

2. The DTT port cross–section dimensions

The launcher dimensions are mainly conditioned by those of DTT toroidal ports (Fig. 2).

Two main launcher approaches have been studied taking into account geometric constraints, assembly and maintenance issues: a plug-in and an in-vessel approach.

The plug-in approach implies a maximum of two columns of straps per launcher, while the in-vessel one allows up to four columns of straps.

The launchers preliminary analyses have been done with the HFSS code. The presently available code version (Ansys Electronic Desktop 2018.1) does not include a plasma model, so that the plasma parameters have been conventionally simulated by a homogeneous dielectric with:

- Relative permittivity $\varepsilon_r = 225$
- Loss tangent tang $\partial = 1.17$ @ 90 MHz.

The values of these parameters have been optimised for having the best fit with the TOPICA code [5] results for a three-straps launcher coupled to a DTT reference plasma (Fig. 3).

* Corresponding author at: Create Consortium Napoli, Italy.
E-mail address: francesco.mirizzi@outlook.it (F. Mirizzi).

https://doi.org/10.1016/j.fusengdes.2023.113788
Received 31 October 2022; Received in revised form 2 April 2023; Accepted 28 April 2023
Available online 2 May 2023

Table 1
DTT Main Characteristics.

Magnetic Field B_0	6 T
Plasma Current I_p	5.5 MA
Major Radius R_0	2.19 m
Minor Radius a	0.7 m
Max Pulse Length	100 s

Between the launcher mouth and the dielectric, a 60 mm vacuum layer has been inserted to account for the SOL coupling conditions.

3. Plug–in launcher topologies and performances

As a first step, flat straps have been considered.
Four main plug–in launcher configurations have been analysed:

- Two parallel straps (Fig. 4a)
- Two antiparallel straps (Fig. 4b)
- Four parallel straps arranged in two columns (Fig. 4c)
- Six parallel straps arranged in two columns (Fig. 4d)

Initial simulations, to preliminarily optimise launcher geometric parameters, have been done without Faraday Screen (FS) and vacuum layer between launcher and plasma.

The main analysed parameters are: the strap width, the distance of the strap front branches from the box back–wall and the vertical position of the coaxial cables along the height of the strap rear branches.

The performance of the four launchers in terms of reflection coefficients S_{nn} in dB, with $0 - \pi$ phasing between the two colums of straps. are summarized in Table 2. These coefficients have been determined at the input of feeding coaxial cables having characteristic impedance $Z_0 = 30\ \Omega$. The resulting values at three representative frequencies of the foreseen frequency range are given in Table 3.

According to this table, the four parallel straps launcher has the better performances in term of reflection coefficients. The six straps launcher, on the converse, has the worst ones.

3.1. Poloidal magnetic fields

Results of the HFSS simulations in term of magnetic field generated by the launchers on their vertical symmetry planes are reported in Figs. 5 and 6.

Launchers with parallel and anti-parallel straps have asymmetric H-fields with reference to their horizontal midplane, while the launcher with four parallel straps, arranged in two rows and two columns, has symmetric H-fields.

Also the six straps launcher has a symmetric H-field referred to its horizontal midplane (Fig. 6), but it presents very high H-fields within the straps.

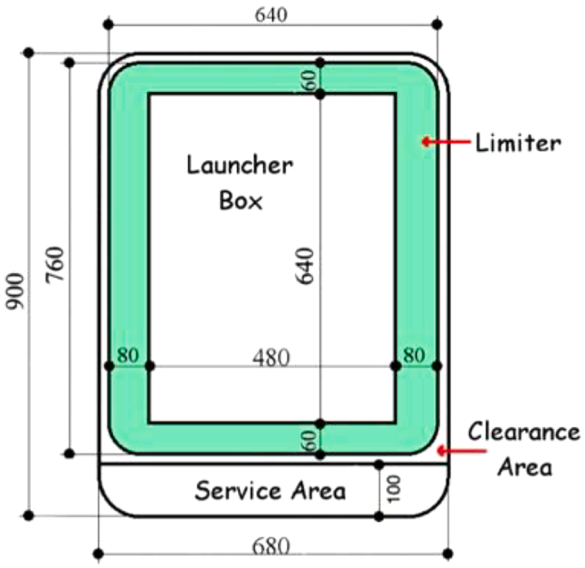

Fig. 2. DTT port cross-section sizes.

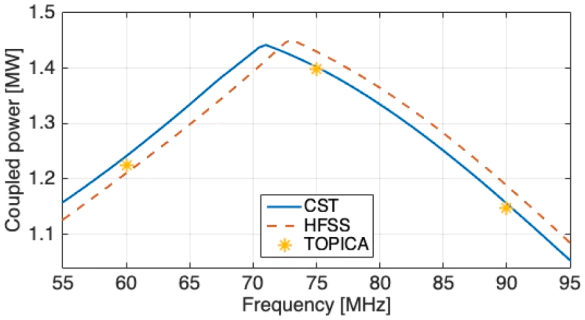

Fig. 3. Benchmark of HFSS and CST simulations with homogeneous dielectric against TOPICA results for a three-strap antenna in front of a DTT reference plasma.

4. Array of four parallel straps

The four parallel straps model with FS and vacuum layer (Fig. 7) has been then further analysed.

The main results, in terms of reflection coefficients S_{nn}, compared to those without FS and vacuum layer, are shown in Table 3, where the related reflected to incident power ratios P_R/P_I are also given

A relevant increase of the reflection coefficients is determined by both the presence of the FS and the interposition of a vacuum layer between launcher and dummy plasma.

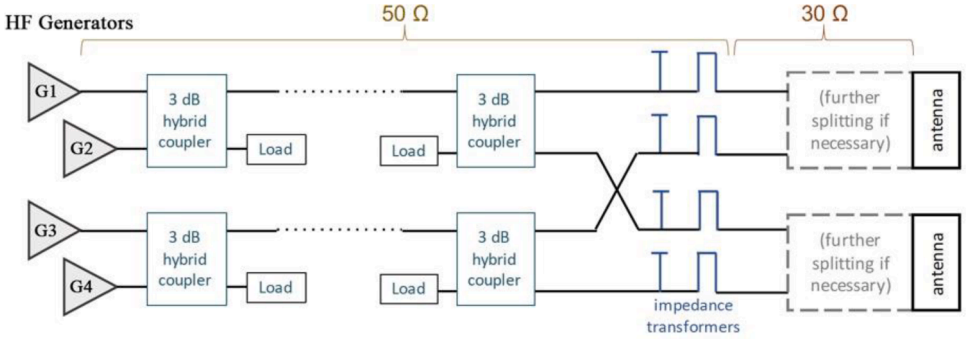

Fig. 1. ICRF system for DTT schematic.

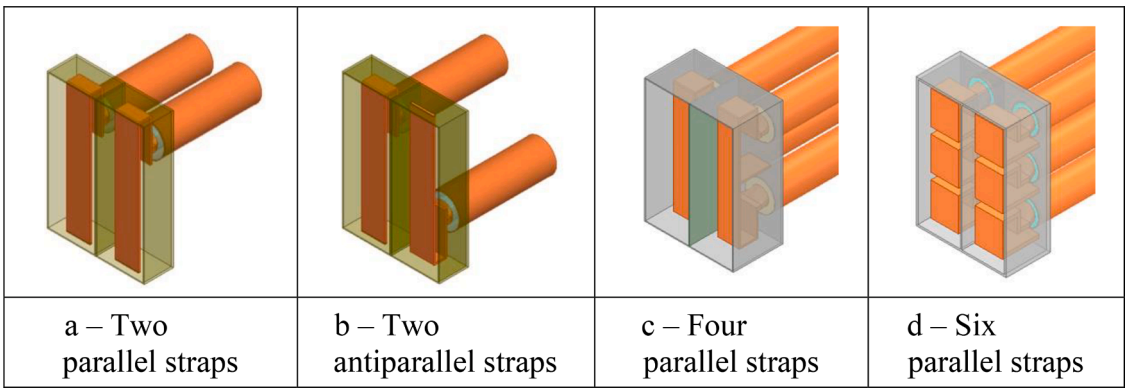

Fig. 4. a Two parallel straps. b – Two antiparallel straps. c – Four parallel straps. d – Six parallel straps.

Table 2
Reflection Coefficients S_{nn} [dB] of the four launchers.

Launcher Type	Frequency		
	60 MHz	75 MHz	90 MHz
Two Parallel/Antiparallel Straps	−1.80	−2.14	−2.37
Four Parallel Straps	−2.13	−2.75	−3.54
Six Parallel Straps	−0.39	−0.48	−0.52

Table 3
Four parallel straps launcher. Main analysis results.

	Plasma Only		Plasma + FS + Vac Layer	
f [MHz]	S_{nn} [dB]	P_R/P_I [%]	S_{nn} [dB]	P_R/P_I [%]
60	−2.13	61	−0.50	89
75	−2.75	53	−0.57	88
90	−3.54	44	−0.69	85

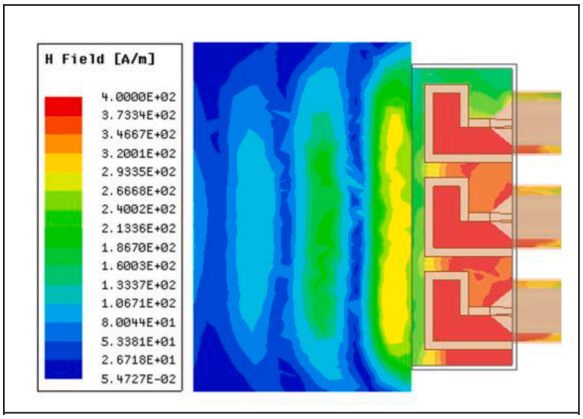

Fig. 6. Six Straps H–Field.

The cross–couplings between the four straps are given in Table 4. The highest values are obtained for the couple of straps on the same columns.

5. Resonant double strap launcher

A double resonant strap launcher [6] with FS and a 60 mm thick vacuum layer (Fig. 8) has been analysed.

Two radially moveable tuning units, made by two copper flat plates, are positioned on the back of the straps. In this way two independent resonant circuits are obtained. The two tuning units are jointly moved by changing their shafts length. For each shaft length the launcher reflection coefficients (Fig. 9) have a main resonant peak which amplitude increases with the shaft length, while the resonant frequency decreases.

Secondary resonant peaks, in the frequency range 101 – 105 MHz, are also noticed. They correspond to the monopole resonance frequency of the strap, depending on the strap length, slightly influenced by the position of the tuning metallic plate. The cross-coupling between the two straps (Fig. 10) is also influenced by the distance between straps and tuning units.

The cross–coupling increases with the frequency, but generally is below −30 dB Two peaks, at about −20 dB, are present at 76 MHz and

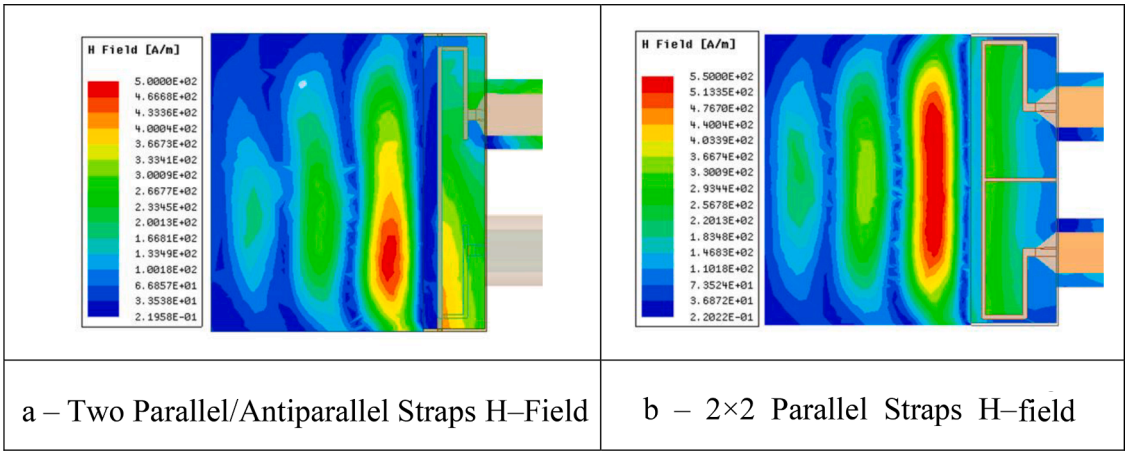

Fig. 5. a Two Parallel/Antiparallel Straps H–Field. b – 2 × 2 Parallel Straps H–field.

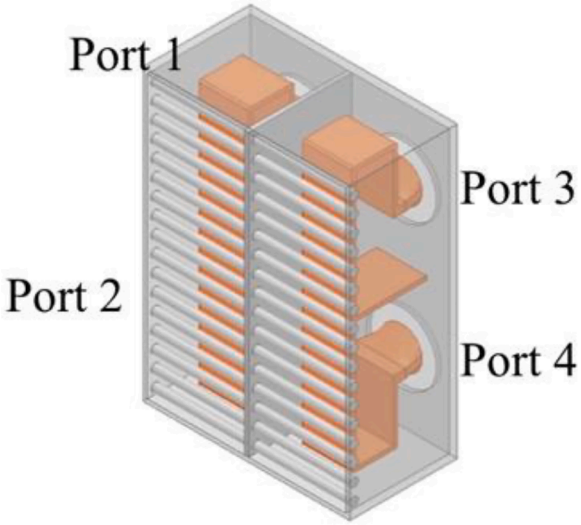

Fig. 7. Four parallel straps with Faraday screen.

Table 4
Four Parallel Straps Launcher. Cross–coupling.

Frequency [MHz]	$S_{12} = S_{34}$ [dB]	S_{13}=S_{24} [dB]	$S_{14} = S_{23}$ [dB]
60	−11.72	−60.93	−60.99
75	−11.55	−64.73	−64.74
90	−11.02	−68.25	−67.96

84 MHz.

As for the reflection coefficients, secondary cross-coupling peaks are noticed in the range 100 – 105 MHz, little influenced by the position of the tuning units.

A possible extension to a four straps launcher is possible, while the extension to three straps one is problematic, unless the three positioning shafts are independently controlled. A weakness of the resonant strap launcher is the relatively high electric fields between the tuning units and the straps. At 60 MHz, where the distance between straps and tuning units is the shortest, the simulation gives a maximum value of about 1.5 $\times$ 10^6 V/m (Fig. 11), for an input power of 600 kW.

Therefore, this launcher configuration needs practical tests on existing ICRF test–bed before being considered as a possible launcher for DTT.

6. The three double strap array

A three double strap array (Fig. 12a) has been also analysed. This configuration has shown good performances on ASDEX Upgrade [7]. In particular it allows the minimization of the parallel RF electric field in the far scrape–off layer (SOL).

Given the DTT port sizes, this array can only be assembled in the in-vessel configuration. For the same reason, to reduce the space taken up by the coaxial cables in the port, the configuration of the side straps is different from that of the central one. Assuming the port assignment in Fig. 12b, the results in terms of S parameters are reported in Table 5.

The table shows bad performances of the lateral straps in terms of reflection coefficients and a very strong cross coupling between the two central straps. Nevertheless, it allows for a lower power density than two-straps antennas owing to the larger radiating area and for the minimization of spurious electric fields in the SOL by properly balancing wave amplitude and phase in the straps.

Diagrams of minimum conductance G_{min} and maximum voltage V_{max} for this launcher are given in Fig. 13.

From these diagrams it is evident that V_{max} never exceeds the safe value of 35 kV.

7. Future work

The analysis is continuing by considering the real curved model of the three double strap array and by completing the model with a suitable local limiter. Once optimized the model by both HFSS and CST–MWS, it

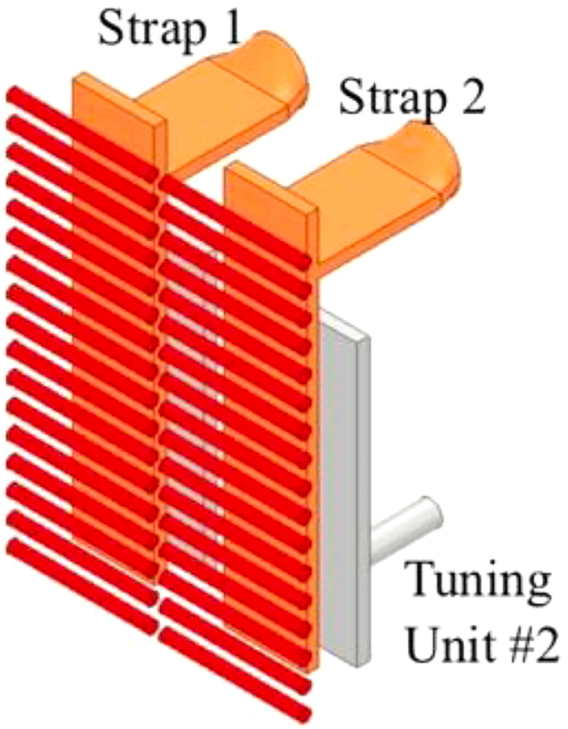

Fig. 8. Resonant double strap launcher.

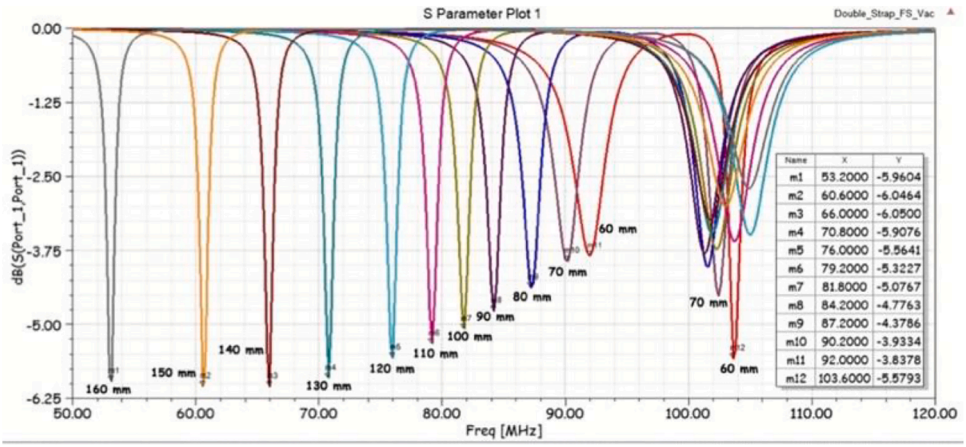

Fig. 9. Resonant Launcher, Reflection Coefficients.

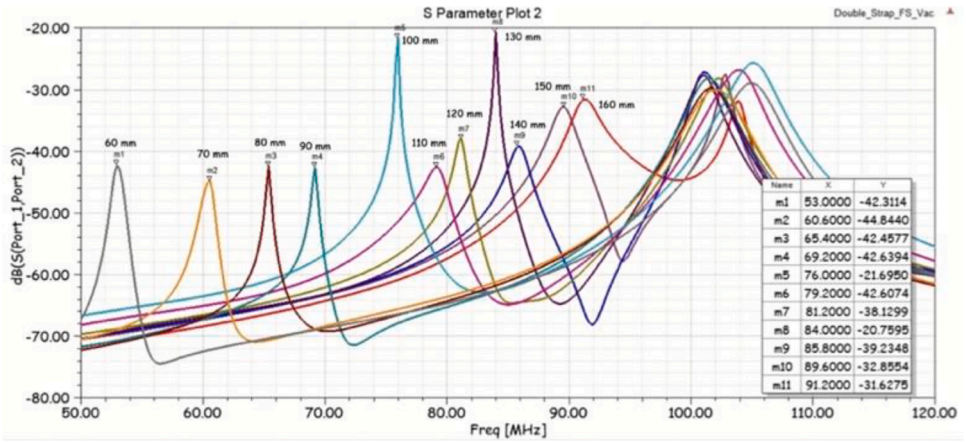

Fig. 10. Resonant Launcher, Cross–coupling Coefficients.

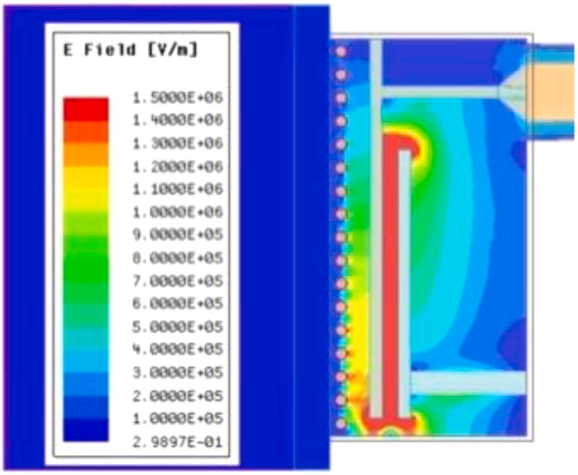

Fig. 11. Electric field between strap and tuning unit at 60 MHz.

will be analysed by TOPICA and by COMSOL Multiphysics, for which a more realistic plasma model has been developed.

8. Conclusions

Several launcher options have been assessed and analysed with the HFSS code to identify the most suitable one for DTT.

The performances of the most attractive options have been also cross–checked with other codes such as CST–MWS, COMSOL Multi-physics [8] and TOPICA [5] obtaining similar results.

The tuneable self-resonant antenna undoubtedly appears as the most promising concept, but it requires further investigation and R&D work, so that it can be only pursued on a longer timescale for a future second couple of DTT launchers. amongst the considered traditional solutions, the best candidate is the 3-straps concept with four feeds, folded lateral straps and end-fed centre-grounded central strap.

Declaration of Competing Interest

The authors declare that they have no known competing financial interests or personal relationships that could have appeared to influence the work reported in this paper.

Data availability

Data will be made available on request.

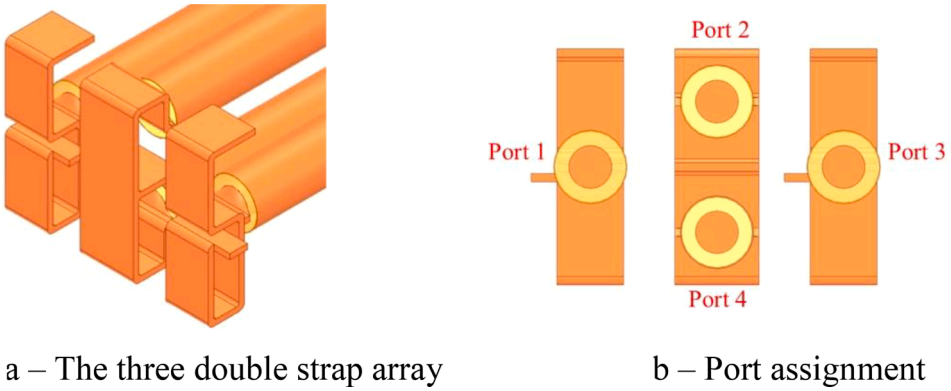

Fig. 12. a The three double strap array. b – Port assignment.

Table 5
Three double–strap launcher. S–parameters.

Frequency [MHz]	$S_{11} = S_{33}$ [dB]	$S_{22} = S_{44}$ [dB]	$S_{12} = S_{21}$ [dB]	$S_{13} = S_{31}$ [dB]	$S_{24} = S_{42}$ [dB]
60	−0.13	−0.73	−47.84	−57.73	−8.77
75	−0.19	−1.00	−45.99	−55.17	−7.48
90	−0.26	−1.27	−44.22	−53.06	−6.50

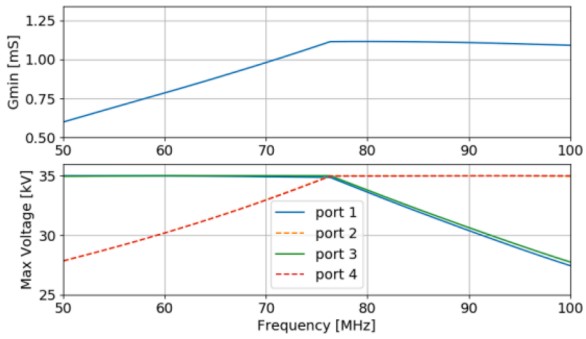

Fig. 13. V_{max} and G_{min} vs frequency for the three straps launcher.

Acknowledgments

This work has been carried out in the frame of DTT activities. The authors are very grateful to all the DTT S.C. a r.l. colleagues for their precious contribution.

References

[1] R. Martone, R. Albanese, F. Crisanti, A. Pizzuto, P. Martin, DTT Divertor Tokamak Test Facility, Interim Design Report (Green Book), ENEA, 2019 (ISBN 978-88-8286-378-4)April.
[2] A. Cardinali, et al., Study of ion cyclotron heating scenario and fast particle generation in the Divertor Tokamak Test (DTT) facility, Plasma Phys. Control. Fusion 62 (2020), 044001.
[3] G. Granucci, The additional heating systems of DTT addressing issues for DEMO HCD Systems, in: Proceedings of the 32nd Sympusium on Fusion Technology, 2022.
[4] S. Ceccuzzi, et al., Conceptual definition of an ICRF system for the italian DTT, Fus. Eng. Des. 146 (2019) 361–364.
[5] V. Lancellotti, et al., TOPICA: an accurate and efficient numerical tool for analysis and design of ICRF antennas, Nucl. Fusion 46 (2006) S476–S499.
[6] D. Milanesio, et al., A self-resonant plug-In IC antenna for DTT, in: Proceedings of the 24th Topical Conference on Radio-frequency Power in Plasma, 2022.
[7] V. Bobkov, et al., Making ICRF power compatible with a high–Z wall in ASDEX Upgrade, Plasma Phys. Control. Fusion 59 (2017), 014022.
[8] G. Torrisi, et al., Development/Extension of a COMSOL full–wave anisotropic model for the ICRH heating, in: Proceedings of the 24th Topical Conference on Radio-frequency Power in Plasma, 2022.